AD-A047 979 AERONAUTICAL RESEARCH ASSOCIATES OF PRINCETON INC N J F/G 13/2
THE IGNITION, COMBUSTION, AND RADIANT INTENSITY OF SPHERICAL CL--ETC(U)
APR 77 P C PETERSEN, E S FISHBURNE, M E NEER F33657-76-C-0315

UNCLASSIFIED ARAP-291 NL

| OF |
AD
A047979

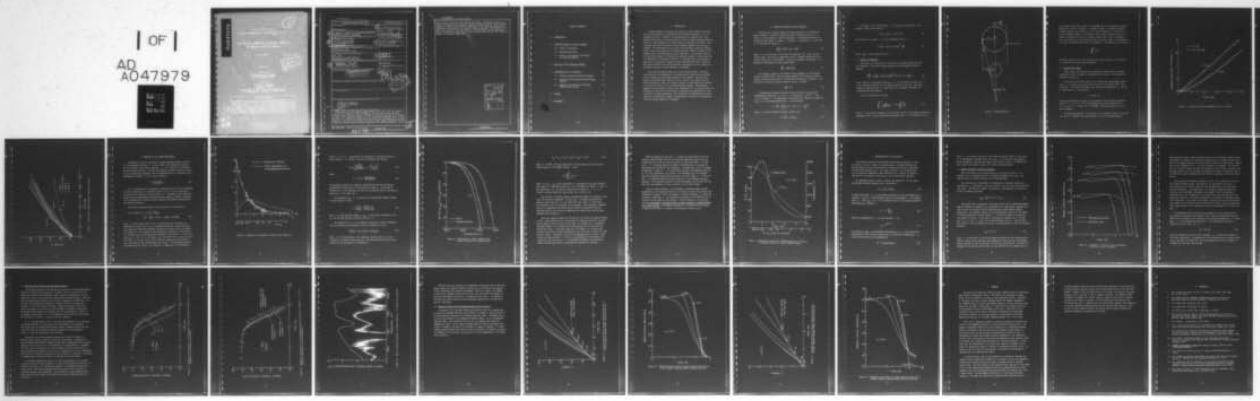

END
DATE
FILMED
1 -78
DDC

A.R.A.P. REPORT NO. 291

AIR FORCE CONTRACT NUMBER F33657-76-C-0315, ITEM 0002

THE IGNITION, COMBUSTION, AND RADIANT INTENSITY OF SPHERICAL CLOUDS OF HYDROGEN

FINAL REPORT

APRIL 1977

Prepared For

FOREIGN TECHNOLOGY DIVISION
AIR FORCE SYSTEMS COMMAND

Prepared By

PRISCILLA C. PETERSEN
E. STORER PETERSEN
MICHAEL E. KERR
AERONAUTICAL RESEARCH ASSOCIATES OF PRINCETON, INC.
50 WASHINGTON ROAD, PRINCETON, NEW JERSEY 08540

UNCLASSIFIED

SECURITY CLASSIFICATION OF THIS PAGE (When Data Entered)

REPORT DOCUMENTATION PAGE

READ INSTRUCTIONS BEFORE COMPLETING FORM

1. REPORT NUMBER

2. GOVT ACCESSION NO.

3. RECIPIENT'S CATALOG NUMBER

4. TITLE (and Subtitle)

THE IGNITION, COMBUSTION, AND RADIANT INTENSITY OF SPHERICAL CLOUDS OF HYDROGEN.

5. TYPE OF REPORT & PERIOD COVERED

Final Rept
7 Jun 76 - 15 Apr 77

6. PERFORMING ORG. REPORT NUMBER

A.R.A.P. Report No. 291

7. AUTHOR(s)

Priscilla C. Petersen
E. Stokes Fishburne
Michael E. Neer

8. CONTRACT OR GRANT NUMBER(s)

F33657-76-C-0315 Item 0002

9. PERFORMING ORGANIZATION NAME AND ADDRESS

Aeronautical Research Associates of Princeton, Inc.
50 Washington Road
Princeton, New Jersey 08540

10. PROGRAM ELEMENT, PROJECT, TASK AREA & WORK UNIT NUMBERS

11. CONTROLLING OFFICE NAME AND ADDRESS

USAF, AFSC
Aeronautical Systems Division
Wright-Patterson AFB, Ohio 45433

12. REPORT DATE

April 1977

13. NUMBER OF PAGES

38

14. MONITORING AGENCY NAME & ADDRESS (if different from Controlling Office)

ARAP-291

15. SECURITY CLASS. (of this report)

UNCLASSIFIED

15a. DECLASSIFICATION DOWNGRADING SCHEDULE

16. DISTRIBUTION STATEMENT (of this Report)

DISTRIBUTION STATEMENT A
Approved for public release;
Distribution Unlimited

38p.

DDC
RECEIVED
DEC 22 1977
F

17. DISTRIBUTION STATEMENT (of the abstract entered in Block 20, if different from Report)

18. SUPPLEMENTARY NOTES

19. KEY WORDS (Continue on reverse side if necessary and identify by block number)

hydrogen-air combustion
entrainment coefficient
IR radiation
thermals

20. ABSTRACT (Continue on reverse side if necessary and identify by block number)

The manner in which large hydrogen bubbles rise, mix, burn, and radiate is predicted for bubbles of varying diameter, initial velocity, and crosswind velocity using simplified models. The motion of buoyant gas bubbles in general is shown to be accurately described by the simplified entrainment model of Shui and Weyl for a variety of bubble sizes and compositions including small hydrogen bubbles as reported in the Russian literature, large bubbles resulting from the combustion of stoichiometric methane-oxygen mixtures (GEST experiments), and very

DD FORM 1 JAN 73 1473 EDITION OF 1 NOV 65 IS OBSOLETE

UNCLASSIFIED

SECURITY CLASSIFICATION OF THIS PAGE (When Data Entered)

008400

large thermals associated with nuclear explosions. The degree to which the mixing is incomplete on a molecular scale is inferred from the observed volume increase of small hydrogen bubbles immediately after ignition, using pseudo-equilibrium calculations with a partial reaction feature. The accuracy of the model used to predict the time history of IR radiation from hot combustion gases is verified by comparison with the observed radiation from the combustion products of methane-oxygen bubbles.

TABLE OF CONTENTS

1. INTRODUCTION

In many industrial processes and research related efforts, the rapid and reliable disposal of large quantities of gaseous hydrogen is of considerable concern. Currently, two techniques are in general use. The Kennedy Space Center in Florida employs a series of small separate ignition devices to burn hydrogen in an area called the "hydrogen burn pond." This technique was used to dispose of excess hydrogen employed in the Apollo program. The Rocketdyne test facility at Canoga Park, California, employs rather high, large diameter vent stacks with pilot flames to dispose of the hydrogen used in testing space shuttle components. An alternate approach for the rapid disposal of hydrogen also appears possible. Large quantities of hydrogen may be released in "bursts" or "bubbles" which are allowed to mix with air and then are ignited at some predetermined time or altitude. This report explores the various problems associated with the release and subsequent ignition of these "bubbles" of hydrogen.

The effort has been divided into three distinct phases. The first phase involves the formulating of the equations of motion and an analysis of the vertical and horizontal movement of the bubbles. The predicted values are compared with the data of Gorev, Gusev, and Troshin[1] and the GEST experiments[2]. Next, the ignition process is investigated and compared to the data of Gorev et al. for small hydrogen bubbles. The agreement generally is quite good. Finally, the formulation for the infrared radiation estimates in the 2.8 μ band of water is discussed and predictions are compared with the GEST experiments. The technique for estimating the radiant intensity is employed to predict the magnitude of radiation to be expected from the burning "bubbles" of hydrogen.

2. SIMPLIFIED THEORY OF RISING THERMALS

The motion of a buoyant thermal has been explored in the simplified models of Wang[3,4] and Shui and Weyl[5] and can be applied directly to a bubble of gas released in a stable atmosphere. The momentum equation for a spherical gas bubble of radius r, volume V, and density ρ less than ρ_∞ of the ambient medium is:

$$\frac{d}{dt}\left(M + M_v\right)U = \left(\rho_\infty - \rho\right)gV \tag{1}$$

where U is the velocity of the center of mass and $M_v = .5\rho_\infty V$ is the virtual mass. Form drag is neglected since it is small compared with the effective drag due to entrainment. The mass entrainment coefficient α is defined by the equation of mass conservation:

$$\frac{dM}{dt} = \alpha\left(4\pi r^2\right)\rho_\infty U \tag{2}$$

The change in energy of the bubble is due primarily to the internal energy of entrained air, which is large compared to the change in kinetic energy, pressure volume work, or the potential energy due to gravity. Conservation of internal energies together with Eq. 2 yields:

$$\frac{dr}{dt} = \alpha U \tag{3}$$

Following the procedure outlined in Shui and Weyl[5] and using the dimensionless variables, $x = r/r_0$, $u = U/[2r_0/2\alpha(1 - A)^2]^{1/2}$, and $\tau = t/(2r_0/\alpha Ag)^{1/2}$, an expression is obtained which relates the expansion ratio x to the dimensionless time τ after release:

$$\tau = -\frac{u_0}{2} + \frac{1}{2}\left[u_0^2 + x^4 - 4Ax - (1 - 4A)\right]^{1/2} \tag{4}$$

where u_0 is the normalized initial velocity and

$$A \equiv 2\left(\rho_\infty - \rho_0\right)/3\rho_\infty \tag{5}$$

The height of the rising bubble z is directly proportional to the change in radius (see Figure 1):

$$z = \left(r - r_0\right)/\alpha = r_0(x-1)/\alpha \tag{6}$$

The velocity for a given x can be determined from Eq. 3:

$$U = \frac{r_0}{\alpha}\dot{x} = \frac{r_0}{\alpha}\left(2r_0/\alpha A g\right)^{-1/2}\frac{dx}{d\tau} \tag{7}$$

where $dx/d\tau$ can be found from Eq. 4.

2.1 Effect of Crosswind

The effect of a crosswind on the rise of a hydrogen bubble has also been examined. Form drag is again neglected and the momentum equation becomes:

$$v\frac{dM_t}{dt} + M_t\frac{dv}{dt} = v\left(4\pi r^2\rho_\infty\alpha\sqrt{U^2+v^2}\right) + \frac{4}{3}\pi r^3\rho_t\frac{dv}{dt} = 0 \tag{8}$$

where dM_t/dt is determined from Eq. 2, U is the upward velocity, and v is the horizontal velocity of the bubble relative to the air. The small change in upward velocity U associated with increased entrainment in crosswinds has been ignored.

Eq. 8 is integrated to obtain:

$$\int_{v_0}^{v}\frac{dv}{v\sqrt{U^2+v^2}} = -3\rho_\infty\alpha\int_{t_0}^{t}\frac{dt}{r\rho_t} \tag{9}$$

where v starts with a negative value and goes to zero as the bubble approaches windspeed. Eq. 9 can be integrated numerically until v has dropped to 5% of

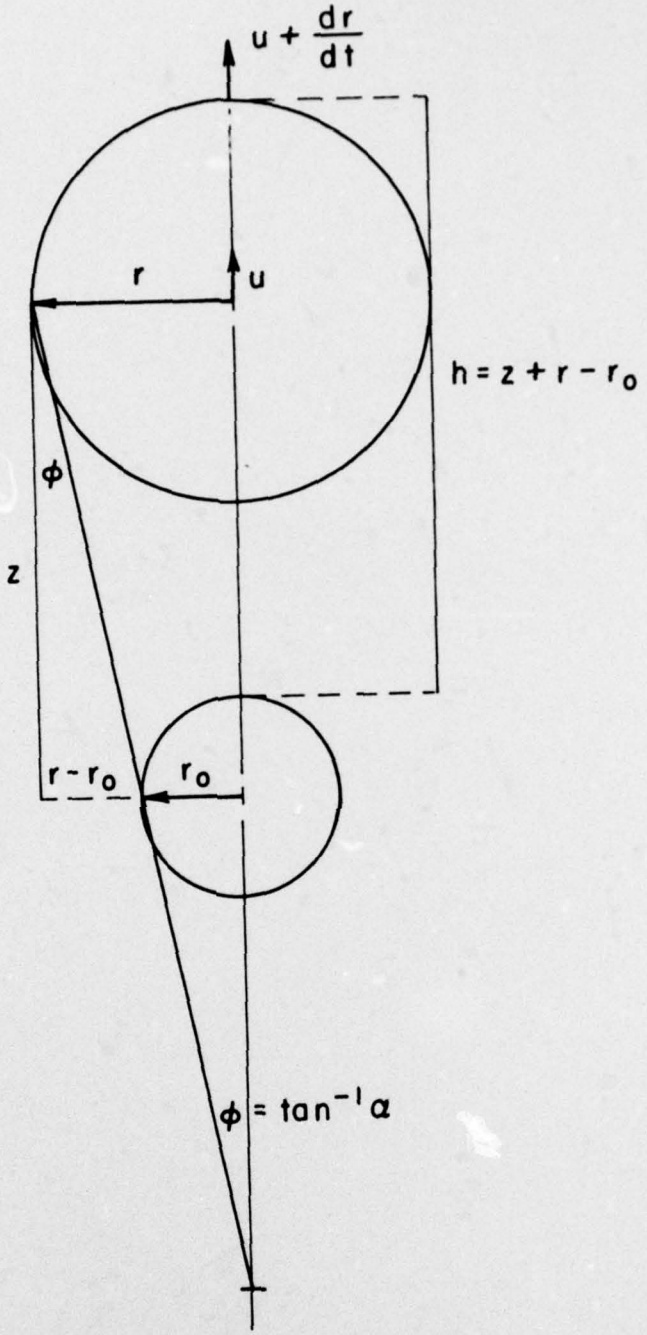

Figure 1. Bubble geometry.

its original value, after which it is assumed that the crosswind no longer affects the rise of the bubble. A bubble 20 meters in diameter reaches a crosswind velocity of 10 mph in only .5 second compared to .2 second for a 1 meter diameter bubble. If the bubble has an initial upward velocity, it reaches crosswind velocity in a slightly longer time. Since entrainment due to crosswind is of such short duration, the major effect of a crosswind is to move the bubble downstream by a distance x according to the relation:

$$x = \int_{t_0}^{t} |v| dt$$

The major effects of a 10 mph crosswind are shown in Figure 2 for bubbles of 1 meter and 20 meters initial diameter.

2.2 Measured Rise Times

Gorev, Gusev, and Troshin[1] have measured the rise times of hydrogen bubbles with initial volumes of approximately 70 liters. Their data are presented in Figure 3.

It should be noted that Gorev et al. define their entrainment coefficient α' in terms of the velocity of the top of the bubble rather than the center. The relation between their empirically determined α' and the α defined by Eq. 2 is therefore:

$$\alpha = \alpha'/(1-\alpha')$$

The two curves shown in Figure 3 are calculated from the model discussed above for $\alpha = .41$ ($\alpha' = .29$) and dimensionless initial velocities of $\Gamma_0 = 0$ and $\Gamma_0 = 4$ where $\Gamma_0 = U_0/\sqrt{r_0 g}$. Data and prediction are in good agreement.

The GEST experiments[2,6] form another set of empirical data in which the rise times of thermals have been measured. In the GEST experiments, a

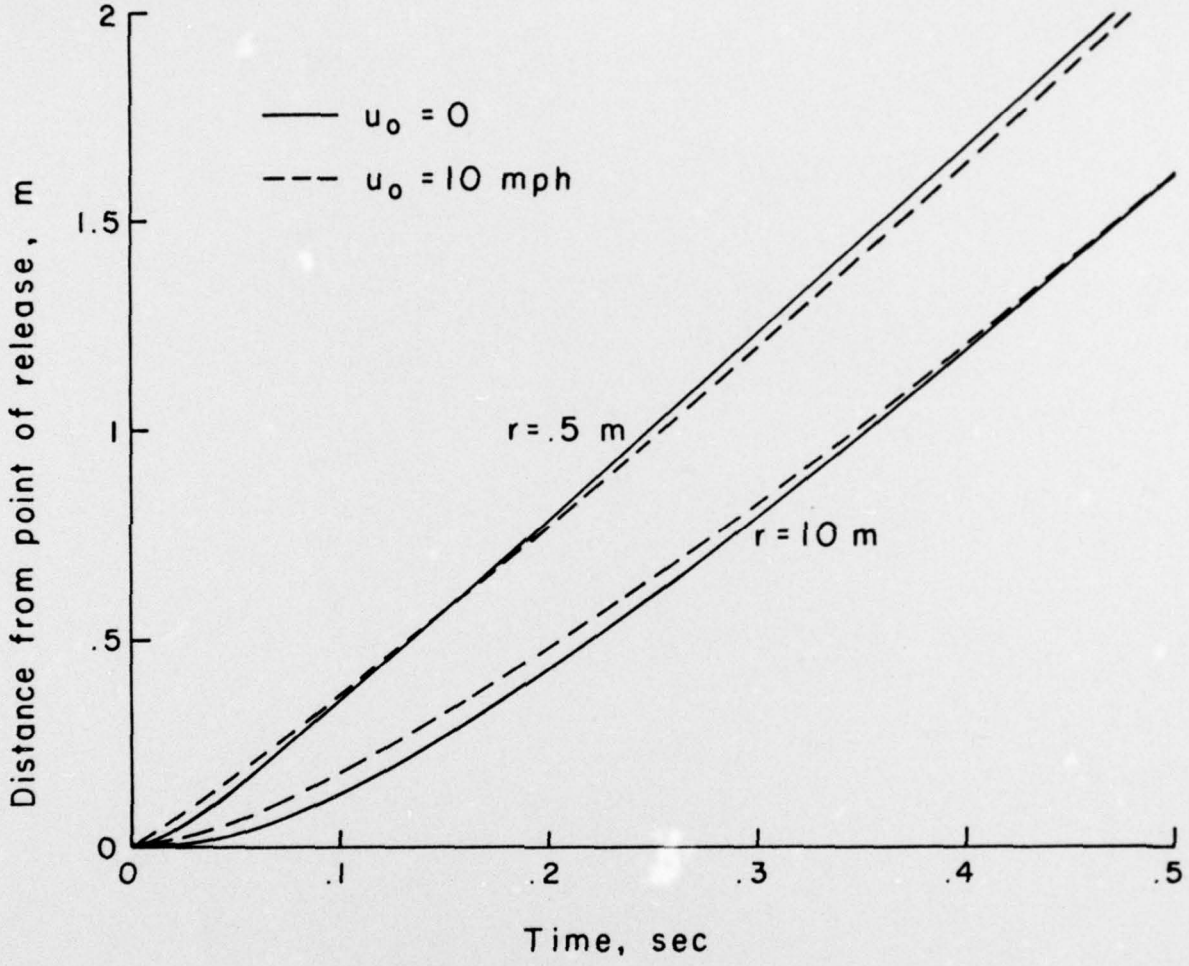

Figure 2. Horizontal bubble displacement due to crosswind.

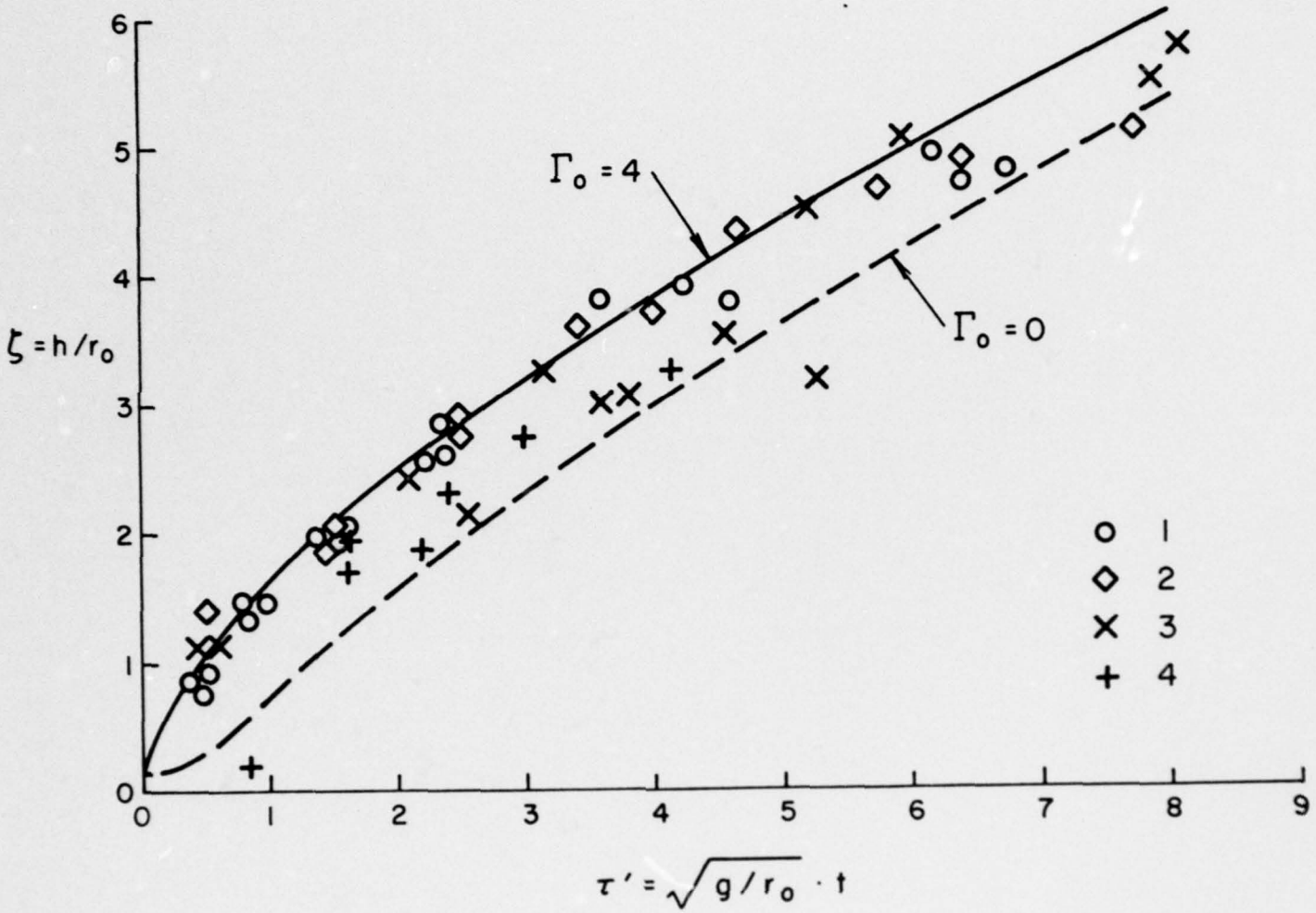

Figure 3. Rise time of H_2 bubbles — from Reference 1.

10 meter diameter mylar balloon filled with a mixture of 1 part CH_4 to 2 parts O_2 was ignited at an altitude of about 150 ft. The height from the ground to the center of the rising toroidal fireball was measured as a function of time after ignition. The data are shown in Figure 4. The theoretical rise rate calculated from the model agrees with the GEST data if the entrainment coefficient is taken to be $\alpha \approx .1 - .12$ instead of .41 used by Gorev et al. Predictions for these values of α are shown in Figure 4. Infrared radiation time histories were also measured in the GEST experiments. It will be shown in a later section that a value of $\alpha = .1 - .12$ is also required to correlate the measured and predicted radiation levels as a function of time. Still another set of data on the rise times of thermals caused by nuclear explosions may be found in Reference 5 (also see References 7 and 8). Apparently, an entrainment coefficient of .25 is required to represent these very large thermals.

2.3 Choice of Entrainment Coefficient for Large H_2 Bubbles

From the three sets of data in the previous section it appears that the simplified model described earlier is adequate to predict the rise times of buoyant gas bubbles if a suitable entrainment coefficient is chosen. Assuming that the observed variations in α are not due simply to experimental error, it appears that small hydrogen bubbles (~ 70 liters) entrain air more rapidly than either very large thermals ($\sim 4 \times 10^6$ cubic meters) from nuclear blasts or large gas clouds from the combustion products of methane-oxygen bubbles which are much hotter than the ambient air.

At present it is not obvious which choice of α is appropriate for large hydrogen bubbles with volumes from $.5 \times 10^3$ to 4×10^3 cubic meters. If one assumes that the initial size of the bubble does not affect the entrainment rate, then larger hydrogen bubbles must behave like their smaller counterparts and α will be close to .41. Operating under this assumption, an α of .41 was used in all the hydrogen bubble calculations presented in this paper. It is important to note, however, that after ignition the hydrogen bubbles may behave similarly to the thermals, requiring a smaller α in that domain.

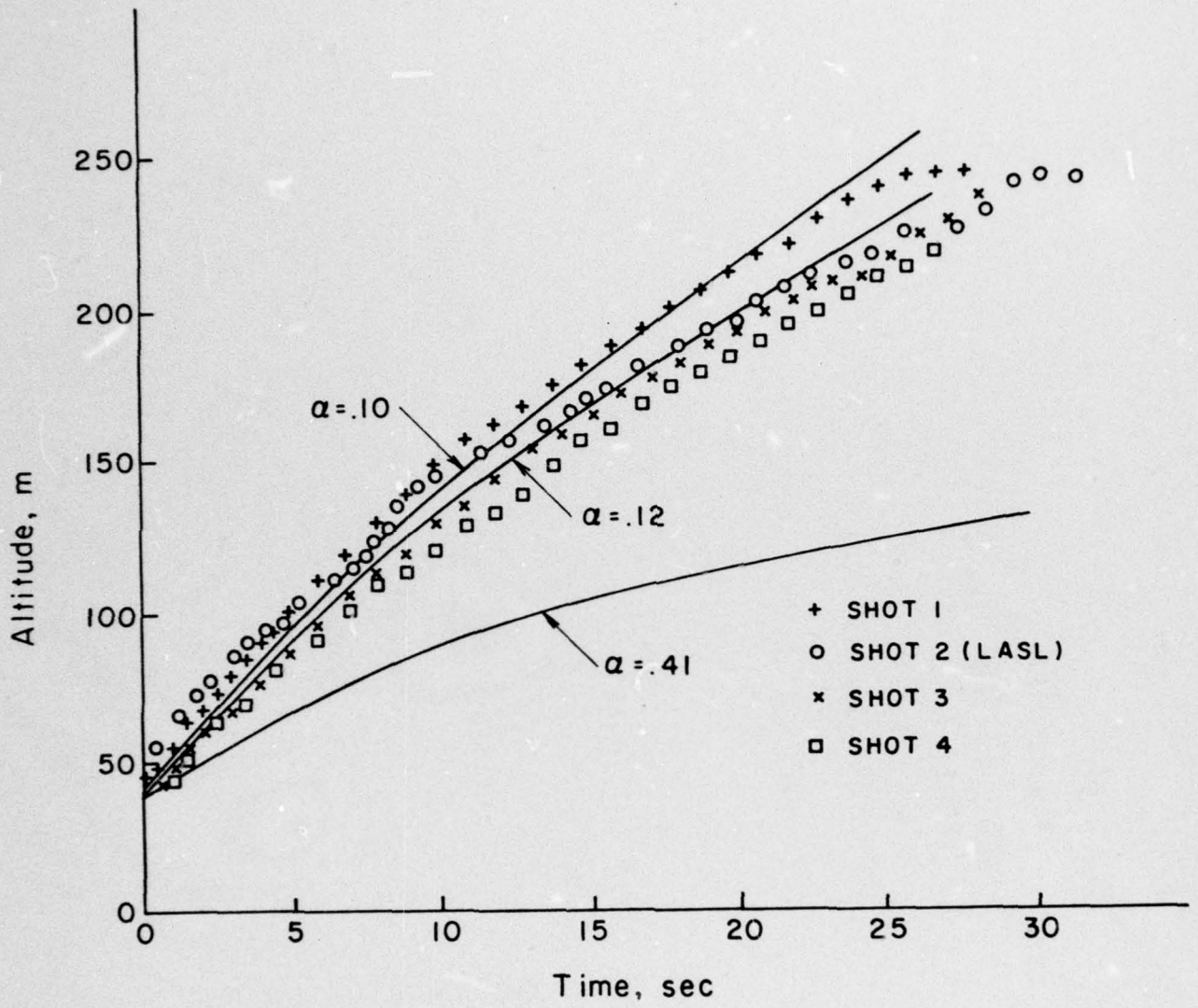

Figure 4. Rise times of methane-oxygen combustion products.

3. MODELING OF THE COMBUSTION PROCESS

In addition to data on the motion of small hydrogen bubbles, Gorev et al. have measured the ratio π of the volume of the combustion products V_2 to the bubble volume before ignition, V, as a function of the height at which ignition occurs. The data is presented in Figure 5 where the solid line is an empirical expression for the expansion data as a function of the nondimensional height $\zeta = h/r_0$ and is given by

$$\pi = \frac{25 - 4.2\zeta}{(.3\zeta + 1)^3} + 1 \tag{10}$$

If it is assumed that the expansion represented by Eq. 10 is independent of initial bubble size, an expanded volume $V_2 = \pi V$ can be assigned to the bubble after ignition at any altitude ζ. Parameters of the combustion process such as percentage of hydrogen burned, degree of mixing, and amount of air entrained after ignition can be obtained from models which maintain the observed expansion.

The overall chemical change within the bubble can be written as

$$1\ H_2 + y\left(.21\ O_2 + .79\ N_2\right) \rightarrow \left(w\beta\right)H_2O + \left(1 - w\beta\right)H_2 + \left(.21y - .5w\beta\right)O_2 + \left(.79y\right)N_2 \tag{11}$$

where y is the overall ratio of air to hydrogen within the bubble as determined in Section 2.0. Due to incomplete mixing on a molecular scale, both unreacted oxygen and unreacted hydrogen may coexist within the bubble. The variable w has therefore been introduced to represent the fraction of the hydrogen which has actually been involved in the reaction. In the fuel lean case w will be ≤ 1.0, while in the fuel rich case w will be $\leq .42y$. The factor β is the ratio of water formed to hydrogen involved and has been introduced to take dissociation into account. An approximate relation was formulated for $\beta(T,R)$ as a function of temperature for equivalence

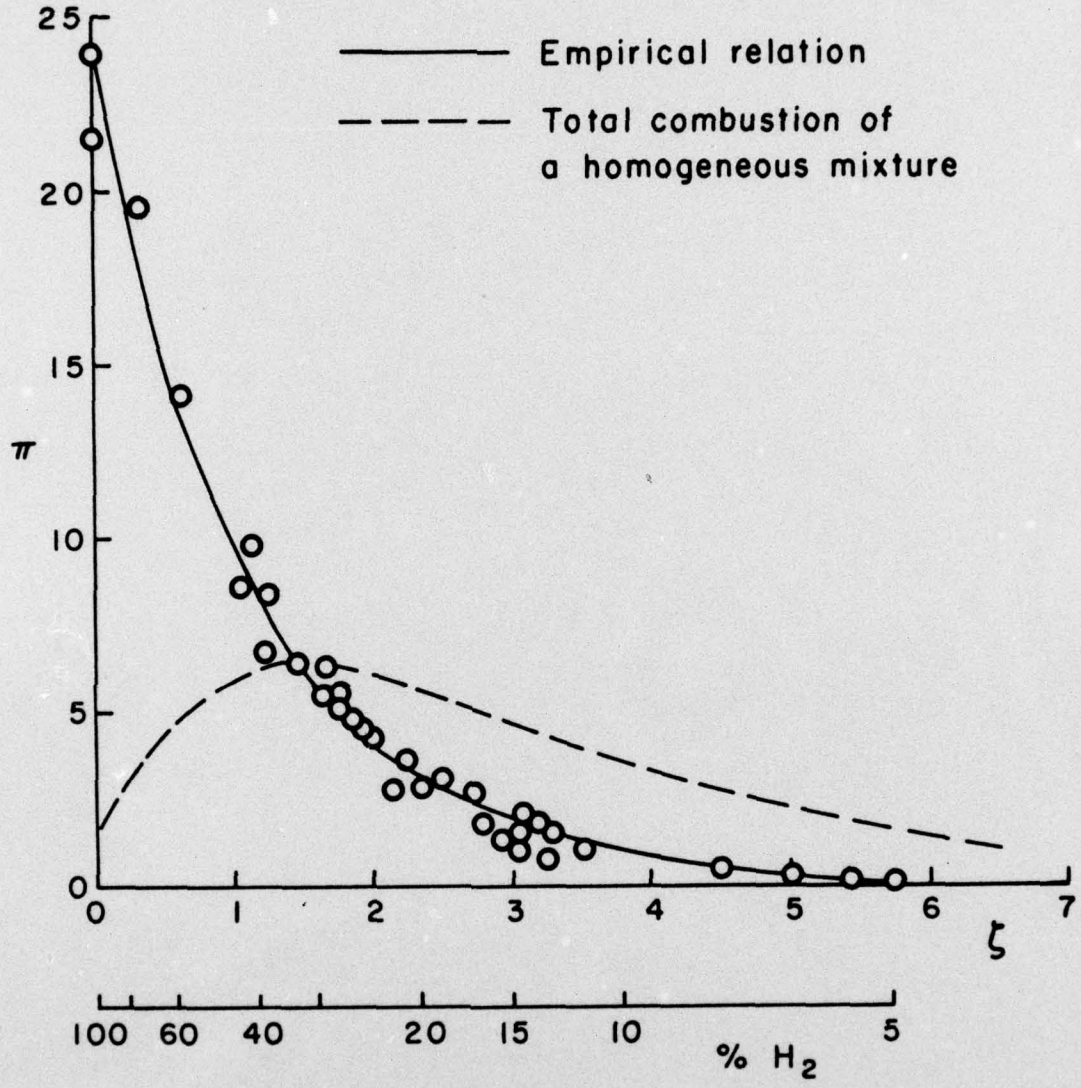

Figure 5. Expansion of hydrogen-air bubbles upon combustion.

ratios $.5 \leq R \leq 4$. The function is normalized to the mole fraction of water formed at $T_2 = 1500°K$ and can be represented as follows:

$$\beta \equiv \frac{\mu_{H_2O}(T_2)}{\mu_{H_2O}(1500°K)} = 1 - \left[\frac{T_2 - k}{2167.}\right]^4 \tag{12}$$

where

$$k = 1277.8 + \frac{826.4|R-1|}{R + 2.375} \tag{13}$$

The agreement between this numerical approximation and the equilibrium calculations of Reference 9 is illustrated in Figure 6. Below 1500°K, virtually all of the hydrogen involved in the reaction will be converted to water and β will equal one.

The expansion ratio π is related to the simplified chemical change via the equation of state

$$\pi = \frac{m_1 T_2}{m_2 T_{STD}} = \frac{\Sigma \mu_{1_i} m_i}{\Sigma \mu_{2_i} m_i} \frac{T_2}{T_{STD}} \tag{14}$$

where m is the molecular weight, T_{STD} is the ambient temperature, and μ_i are the mole fractions derivable from Eq. 11.

The temperature T_2 of the combustion products is found by assuming that the combustion and expansion process is adiabatic so that

$$H_2(T_2) = \Sigma \mu_{2_i} H_i(T_2) = H_1(T_{STD}) \tag{15}$$

where H_2 is the enthalpy of the combustion products and H_1 is the enthalpy of the bubble before ignition. The molar specific heat for each species can be expressed as a polynomial[10]:

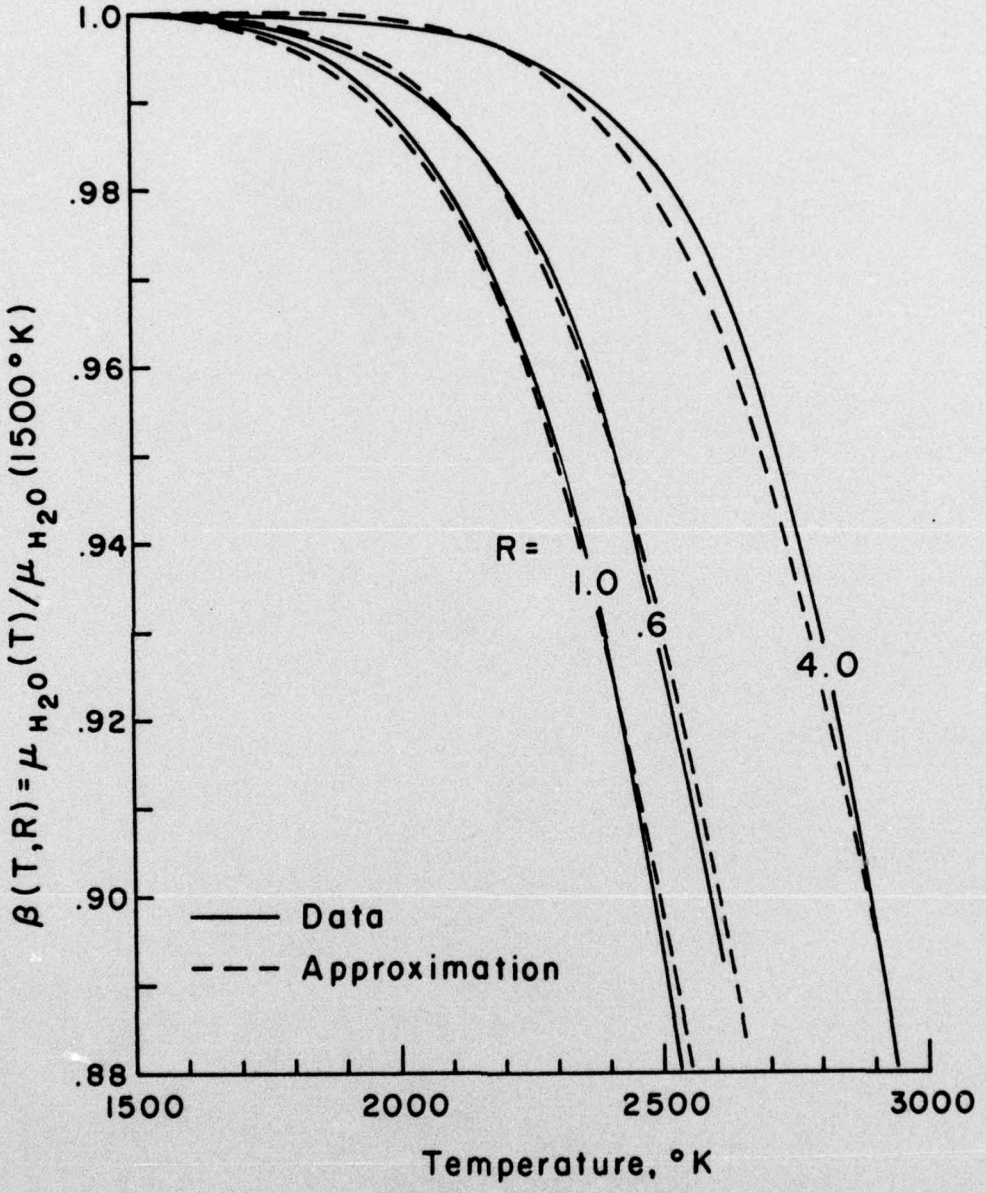

Figure 6. Approximation $\beta(T,R)$ compared with actual fraction of dissociated water.

$$c_{p_i} = L_{1_i} + L_{2_i}\phi + L_{3_i}\phi^2 + L_{4_i}\phi^3 + L_{5_i}\phi^{-2} \qquad (16)$$

where $\phi = T/1000$ and the coefficients are found from curve fits of individual species in the JANNAF tables[11]. Since

$$H_i = \int_{T_0}^{T} c_{p_i} dT + k$$

where $k = L_{6_i}$, H_i can be expressed as a polynomial as well and iterated with respect to temperature until Eq. 15 is satisfied for a given w and y. The temperature T_2 can then be iterated with respect to w or y to obtain a solution which will satisfy both Eq. 14 and Eq. 15.

For the case of complete mixing, hydrogen and oxygen are allowed to burn until one species is depleted. In this case w becomes unity when the bubble is fuel lean and $w = .42y$ when fuel rich, where $y = (V - V_0)/V_0$, the volumetric ratio of entrained air to hydrogen. This simplistic approach leads to an expansion time history which differs considerably from the available data as can be seen by comparing the dashed curve with the Gorev hydrogen data in Figure 5.

There are several reasons why the data do not follow the complete mixing curves. Since sufficient air is entrained for complete combustion (stochiometric mixture ratio) in such a short time (~.5 seconds for a 1 m diameter hydrogen bubble), it is unlikely that the hydrogen and air are mixed on a microscopic scale. In the fuel lean case for example, it is likely that pockets of gas exist in which the mixture ratios are above or below the flammability limits. Therefore, not all of the hydrogen will be burned. Thus, in the fuel lean case the y of Eq. 11 is determined by the volume of entrained air and the value of w is decreased according to the iteration scheme discussed above until the appropriate expansion is obtained.

When the mixture is fuel rich, y cannot be found directly from the expanded volume because the fuel rich mixture apparently reacts with the surrounding air as well as with that which has been entrained[12]. In this case, y is increased beyond the amount of entrained air to include the surrounding air involved in the combustion. Assuming that all of the oxygen is depleted, a value of y is found which satisfies the expansion given by Eq. 14, thus determining $w\beta$ as well. For extremely fuel rich mixtures where the expansion after ignition appears to be very large, w is set to 1 and y is increased beyond the point where all of the hydrogen has been depleted. This procedure accounts for the entrainment of air which does not burn with the hydrogen, but does contribute to the final volume.

Using the above analysis, the percentage of hydrogen burned and the temperature of the combusted mixture as a function of time after release are presented in Figures 7 and 8 for bubbles of initial diameters of 1 meter and 20 meters, respectively. The percentage of hydrogen in the bubble prior to ignition is also shown on the abscissa. From the figures it can be seen that the percentage of hydrogen burned is always greatest if ignited immediately after release. The highest temperature is achieved when the bubble is ignited just before it reaches a stoichiometric mixture ratio.

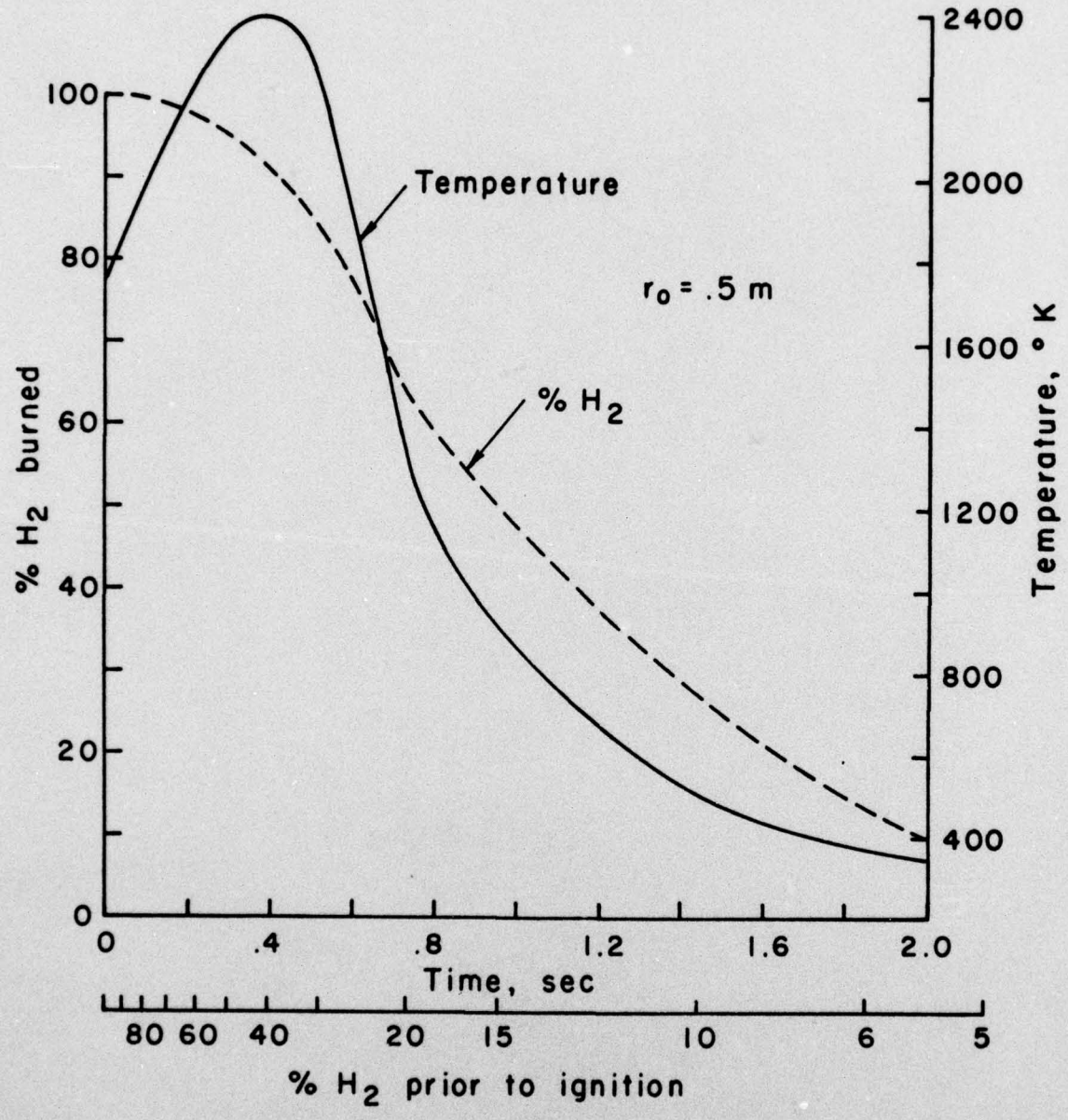

Figure 7. Temperature and percent hydrogen burned as a function of ignition time for a 1 meter diameter bubble.

4. DETERMINATION OF IR RADIATION

The radiation emitted from hydrogen bubbles after combustion is also of interest, both as a means of interpreting the readings obtained from various sensors and as testing models of mixing and cooling by comparison with existing radiation data. Two cases of interest can be identified: (a) the radiation immediately after combustion as a function of ignition time and (b) the radiation time history of the bubble after ignition.

An isothermal model is used to compute the radiation. In this model the infrared radiant intensity can be expressed as

$$J_\lambda = \varepsilon_\lambda R_{0,\lambda}(T) A_{eff} \tag{17}$$

in watts/str/μ where ε_λ is the effective emissivity over the bandwidth of interest, $R_{0,\lambda}(T)$ is the blackbody function for wavelength λ and temperature T, and $A_{eff} = \pi r^2$ is the effective area of the radiating bubble[13]. The emissivity is given as:

$$\varepsilon_\lambda = 1 - \prod_{i=1}^{n} \tau_i \tag{18}$$

where the transmissivity τ_i of each species i is:

$$\tau_i = e^{-W_i/d_i} \tag{19}$$

and $\left(W_i/d_i\right) = k_i X_i$ in the weakline approximation. k_i is the absorption coefficient in the 2.8 micron region and is a function of temperature. X_i is the optical depth and is expressed as

$$X_i = \mu_i p_\infty L_{eff} T_{STD}/T_2 \tag{20}$$

where μ_i is the mole fraction of the radiating species (water in this case), p_∞ is atmospheric pressure (atm), and L_{eff} is the effective path length, Detailed numerical calculations using the band model found in the SPECRA computer code[14] give answers within 10% of this shorthand method.

4.1 Bounds on Radiant Intensity Estimates

Since the bubble is not always mixed on a microscopic scale, it is unlikely that the temperature will be constant throughout the cloud. Two limiting cases of mixing, however, can be distinguished.

One limiting case corresponds to a homogenous, isothermal bubble with temperature T_2 calculated in the last section. The fuel lean case approaches this limit. The effective length is obtained by approximating the bubble as a slab of radiating material:

$$L_{eff} = \frac{4}{3}\pi r^3 / \pi r^2 = 1.33\, r \qquad (21)$$

The second limit corresponds to the most severe case of incomplete mixing where the bubble is assumed to be stoichiometric in some regions, perhaps in a shell around the outside, and the remaining gas is maintained at ambient temperature. The chemical change in the stoichiometric portion of the bubble is treated separately, and the volume V' of these hot gases is found from the equation of state. In the case of hydrogen-air bubbles, Eq. 11 is used with $w = 1.0$ and $y = 2.38$ for the stoichiometric portion. The effective path length of the stoichiometric portion is approximated by a slab of radiating material:

$$L_{eff} = V' / \pi r^2 \qquad (22)$$

where r is the radius of the entire sphere including the cold unmixed gases. Figure 9 shows the two limiting cases immediately after ignition for hydrogen bubbles ignited at various altitudes in their rise time history. Normally the homogenous case yields a lower limit to the radiation and the unmixed case an

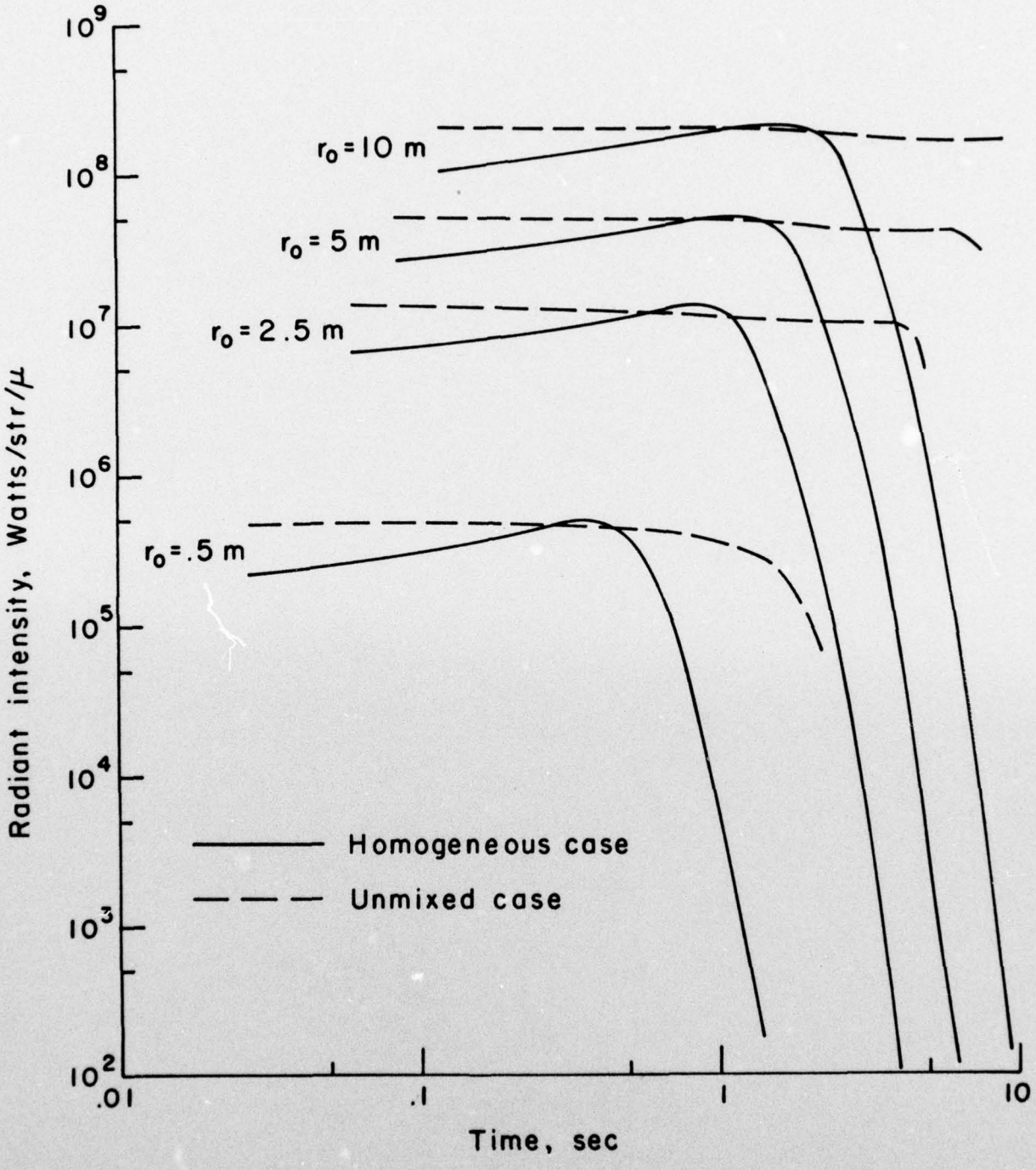

Figure 9. Dependence of initial radiant intensities at 2.8 μm on time of ignition.

upper radiation limit. When the mixture ratio of the homogenous bubble becomes stoichiometric, however, its radiation signature will be slightly higher than that of the unmixed bubbles since dissociation effects are less severe. Bubbles with initial diameters of 1, 5, 10, and 20 meters are examined. The relative effects of initial upward velocity and crosswind on the initial radiation from hydrogen bubbles of 1 and 20 meters in diameter are shown in Figures 10 and 11. The effects are small compared with the radiation dependence on initial bubble radius.

After ignition the bubble continues to rise. As it mixes with cold air the radiation drops rapidly. The moles of air entrained at any time t after ignition can be found using the Shui and Weyl model with appropriate initial conditions. The temperature of the bubble is again determined by iteration on the enthalpy polynomials from JANNAF[11] until the adiabatic expression (Eq. 15) is satisfied for the given ratio of entrained air to hot combustion products. This method assumes that the bubble is thoroughly mixed after combustion. The volume of the bubble from which we derive the effective path length is recalculated from the equation of state at the new temperature, thus taking account of the temperature and species dependence of the specific heat.

An additional effect that must be accounted for in the calculation of the effective temperature is radiative loss. Some of the energy in the hot bubble will be radiated away according to the Stefan-Boltzmann law, $J = \varepsilon\sigma T^4$, where ε is the engineering emissivity[15]. The temperature drop due to radiative loss in a time Δt is:

$$\Delta T = J\Delta t/nc_p \qquad (23)$$

where the temperature drop for each increment Δt is small with respect to the bubble temperature. Recombination of the reacting species, however, would tend to maintain the bubble near the flame temperature until the energy of recombination had been radiated away.

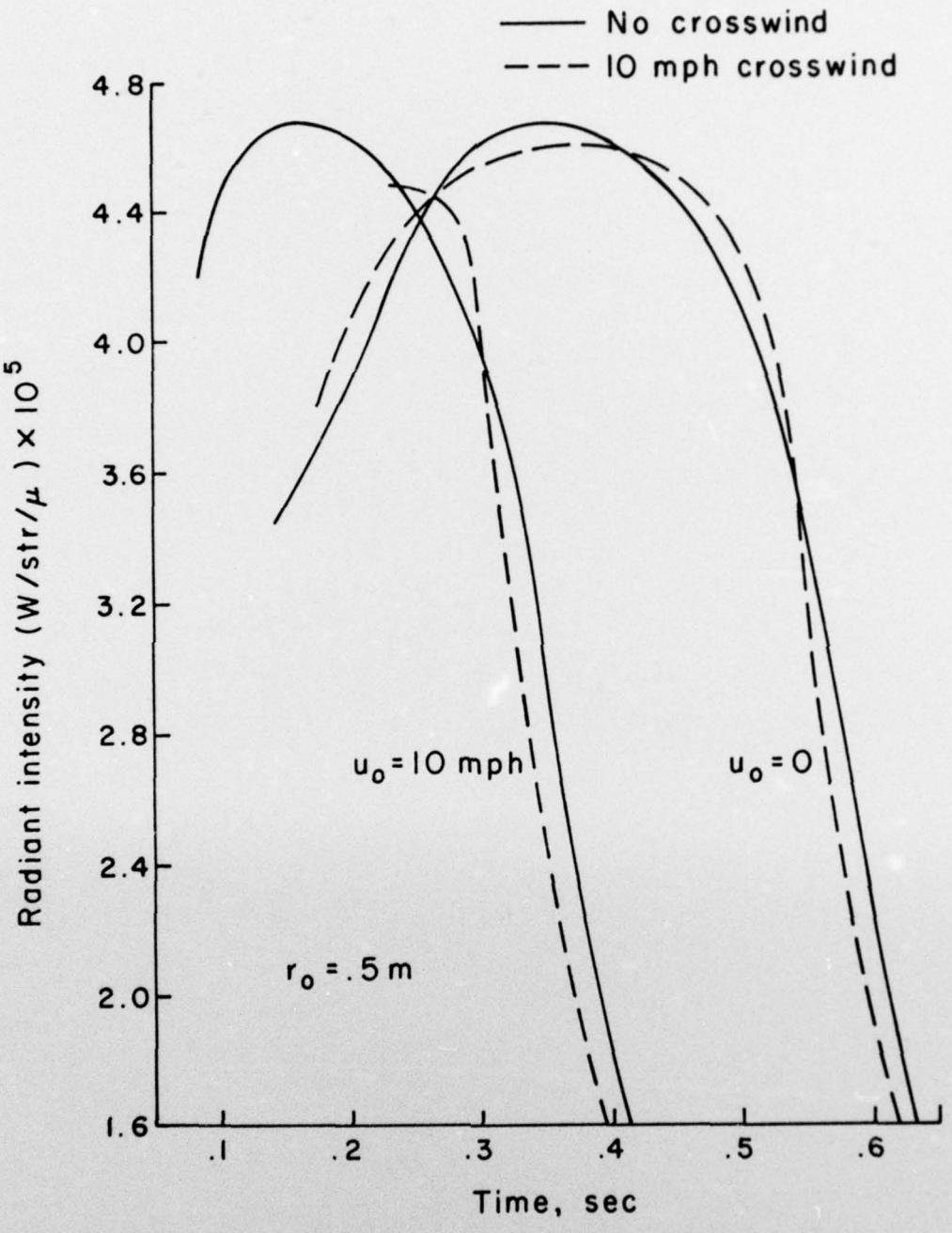

Figure 10. Effect of crosswind and upward velocity U_0 on initial radiant intensities for 1 meter diameter H_2 bubble.

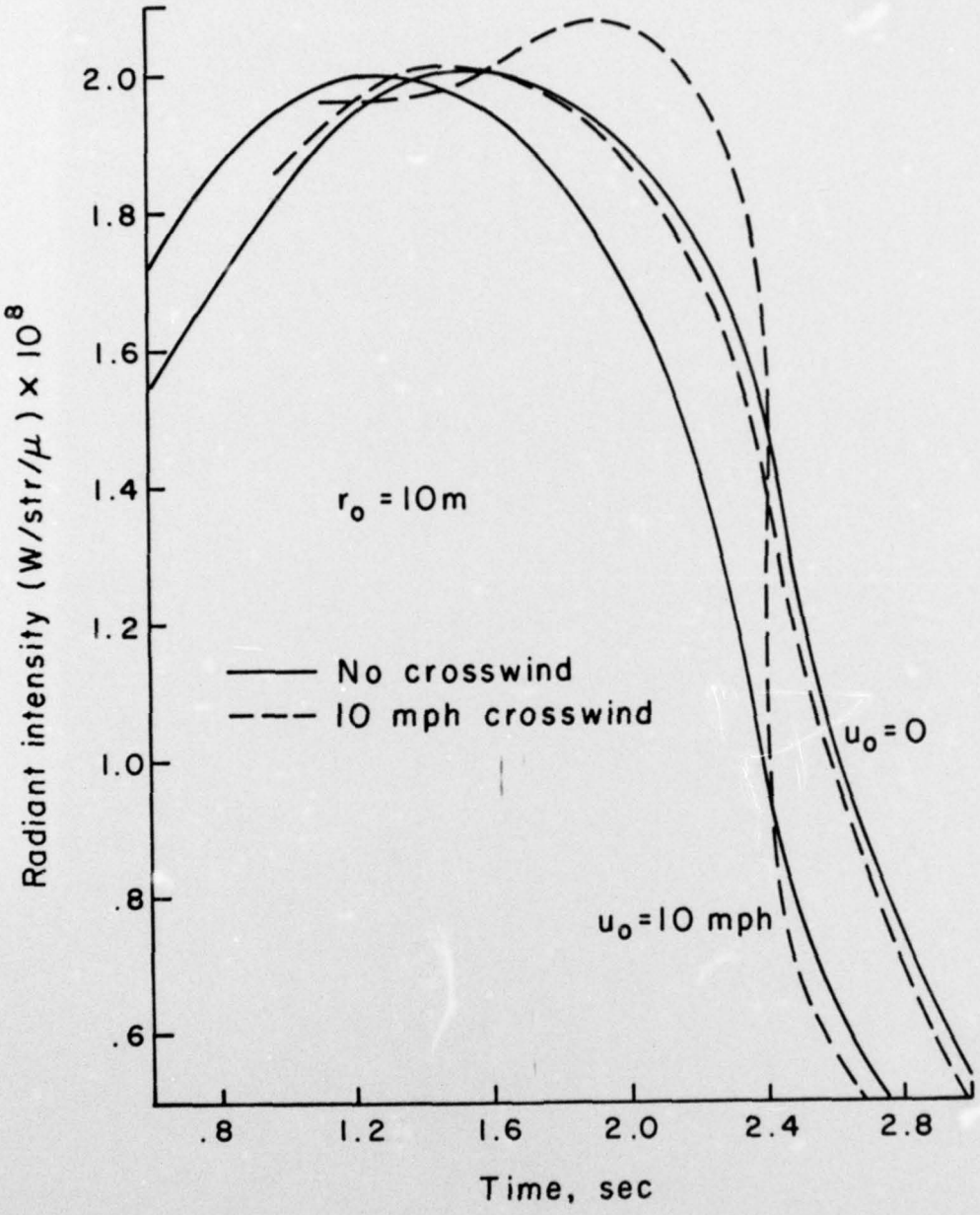

Figure 11. Effect of crosswind and upward velocity U_0 on initial radiant intensities for 20 meter diameter H_2 bubble.

4.2 Radiation from Combusted Methane-Oxygen Bubbles

In the GEST experiments the radiation time history of the methane-oxygen bubble after ignition was measured. In order to test the validity of the simplified radiation model discussed above, radiation estimates for the hot combustion products were obtained by applying the radiation model to stoichiometric methane-oxygen bubbles and the results compared to the GEST data. In our model the atmosphere is assumed to contain .03% CO_2 by volume with a humidity of 20% (1.34% water by volume). Figure 12 presents theoretical curves calculated on the basis of three different entrainment coefficients and neglecting the effects of radiative loss and recombination. Again, an entrainment coefficient of .1 - .12 is suggested since radiation calculations on the basis of a larger α fall off much too rapidly.

As α becomes smaller ($\alpha < .1$), the form drag neglected in our analysis may become important. If form drag is not negligible, the entrainment coefficient for the methane-oxygen bubble could be somewhat smaller ($\alpha = .08$) and still result in a radiation prediction similar to that produced by larger α when form drag effects are included.

Radiative loss and recombination effects are treated in Figure 13. Neither effect greatly changes the radiation time history. Although a 10 meter diameter stoichiometric methane-oxygen bubble immediately after ignition radiates at the rate of 2.02×10^9 watts/str/sec corresponding to a temperature loss rate of 1478°K/sec, the cooler bubble is denser at each point in time and mixes less rapidly with the air. In addition, the rate of temperature decrease due to radiative loss drops to about 10°K/sec in .8 second. Inclusion of recombination reduces the effect of radiative loss even further.

In the GEST experiments, spectra of the radiating bubble in the region from 2400 - 6400 cm^{-1} were recorded at .11 and 5.15 seconds after ignition. In Figure 12 the data at .11 second are compared to the SPECRA band model discussed above. The input parameters were bubble radius, mole fraction of radiating species, and temperature. Since values for these parameters were taken from our simple model, the comparison provides an additional test of the model.

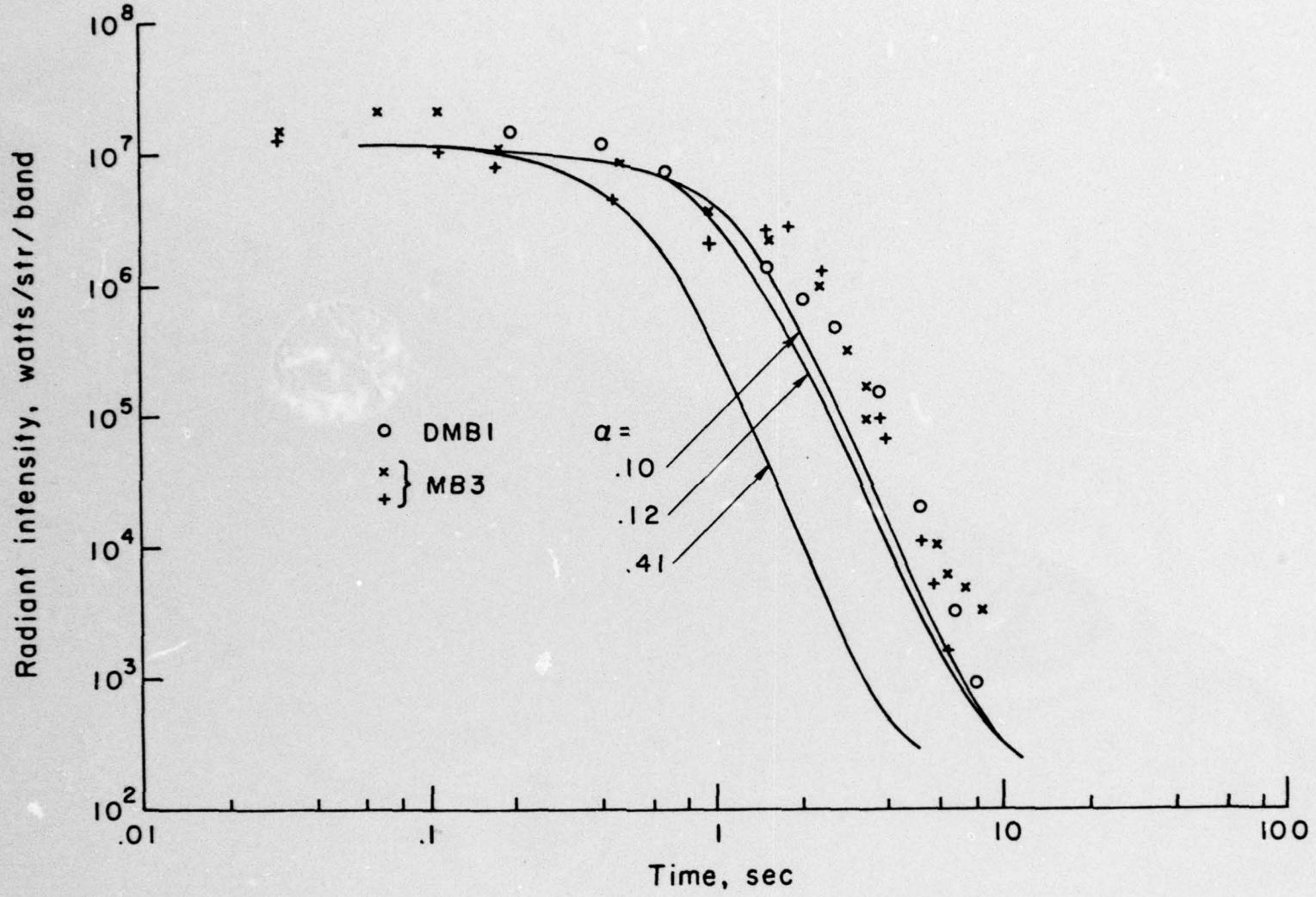

Figure 12. Radiation time history of a stoichiometric CH_4-O_2 bubble after ignition, λ = 2.8 μ. Dependence on entrainment coefficient.

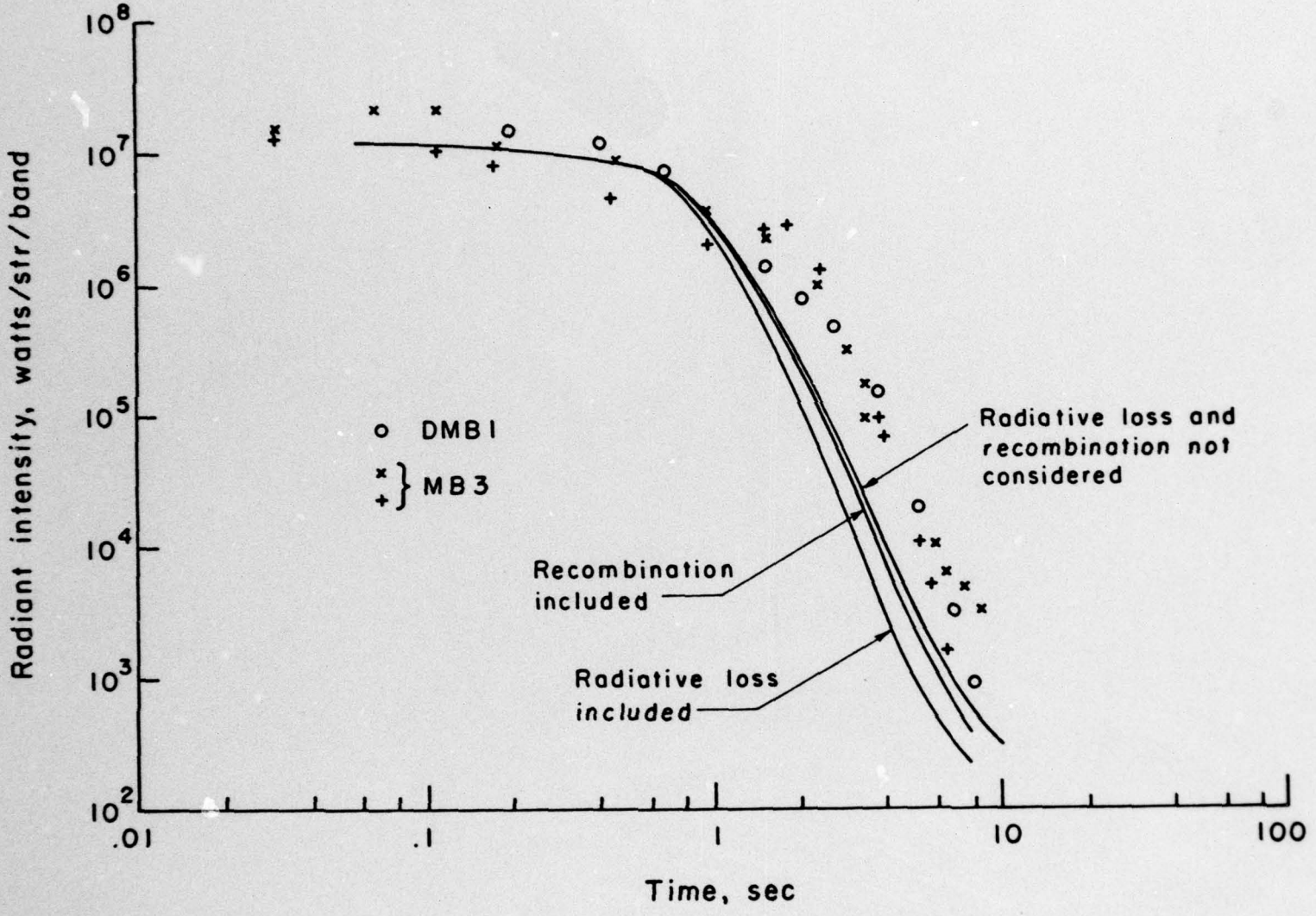

Figure 13. Radiation time history of a stoichiometric CH_4-O_2 bubble after ignition, λ = 2.8 μ. Effect of radiative loss and recombination.

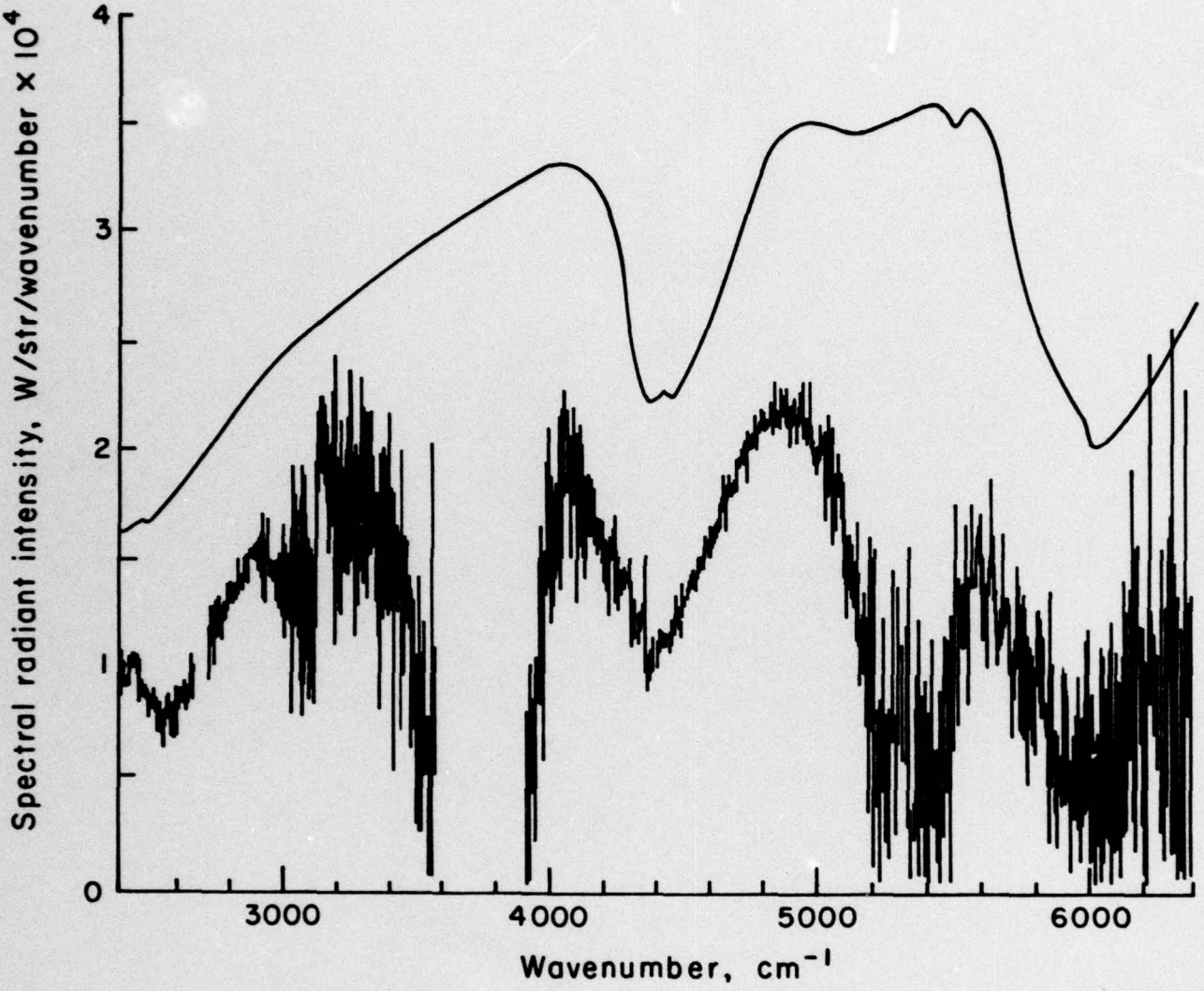

Figure 14. Spectral radiant intensity for CH_4-O_2 bubble at .11 second after ignition.

The data have been corrected for atmospheric absorption, but in some wavelength regions the spectral radiant intensity was so low due to the severity of the attenuation that accurate adjustments could not be made. The SPECRA calculation is somewhat higher than the data, but well within the scatter of the data (see Figures 12 and 13). The same variation with λ is evident in both data and theory except in those wavelength regions where the data were severely attenuated.

4.3 Radiation Predictions for Hydrogen Bubbles After Ignition

In Figures 15-18, the model neglecting radiative loss and recombination is applied to hydrogen bubbles 1 and 20 meters in diameter. Figures 15 and 17 show altitude-time histories for different ignition times. The dashed line is the rise time history of an uncombusted hydrogen bubble. As the uncombusted hydrogen bubble rises and mixes with the air, it rapidly drops below the flammability limit. By the time a hydrogen bubble 20 meters in diameter has risen to a height of 40 meters (10 seconds), it cannot be ignited. A 1 meter diameter bubble reaches this limit in only 2.2 seconds at a height of 2 meters. The rapidity of this process is partially due to the unmixedness of the bubble before ignition.

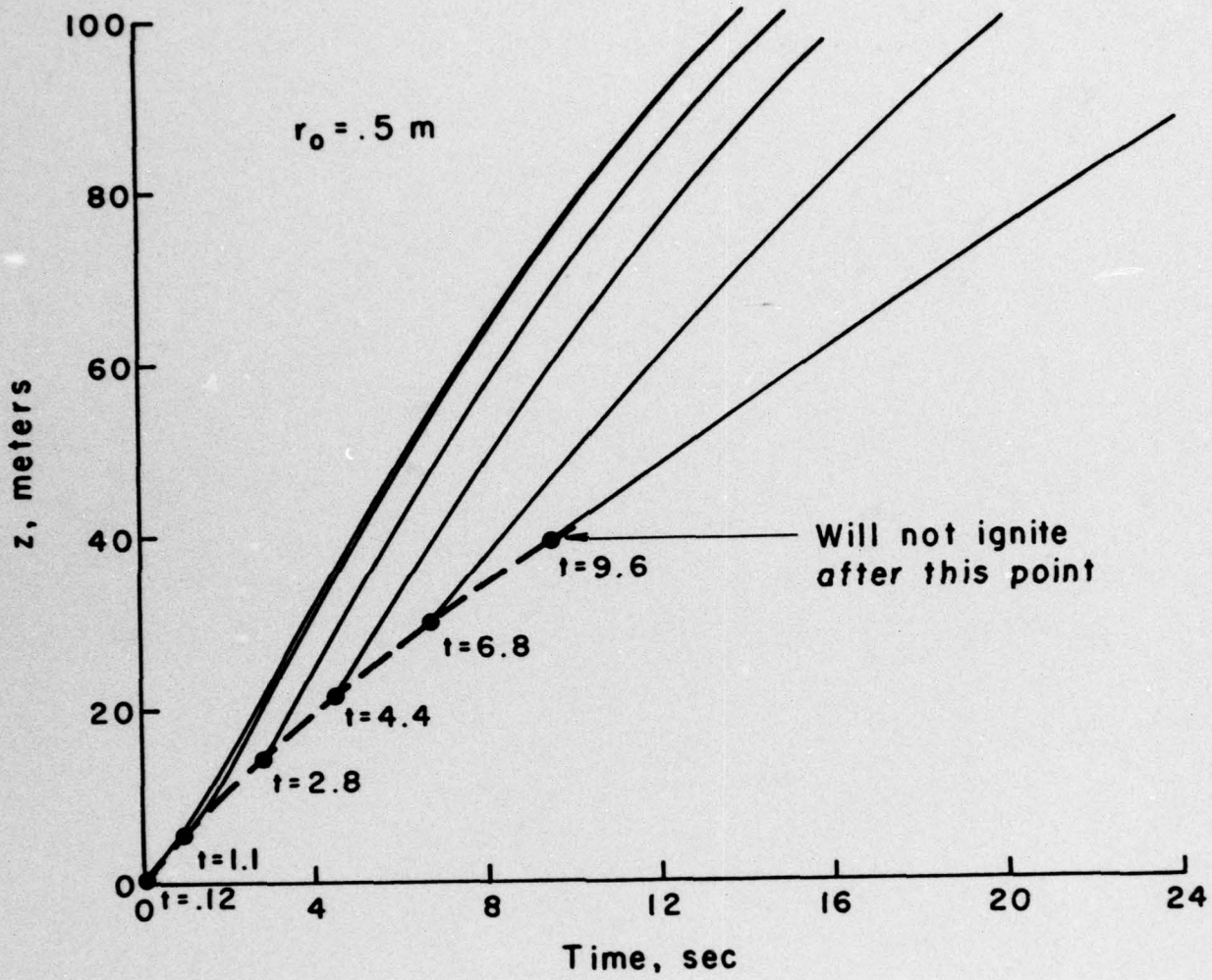

Figure 15. Altitude time history at various ignition points for a 1 meter diameter hydrogen bubble starting from rest.

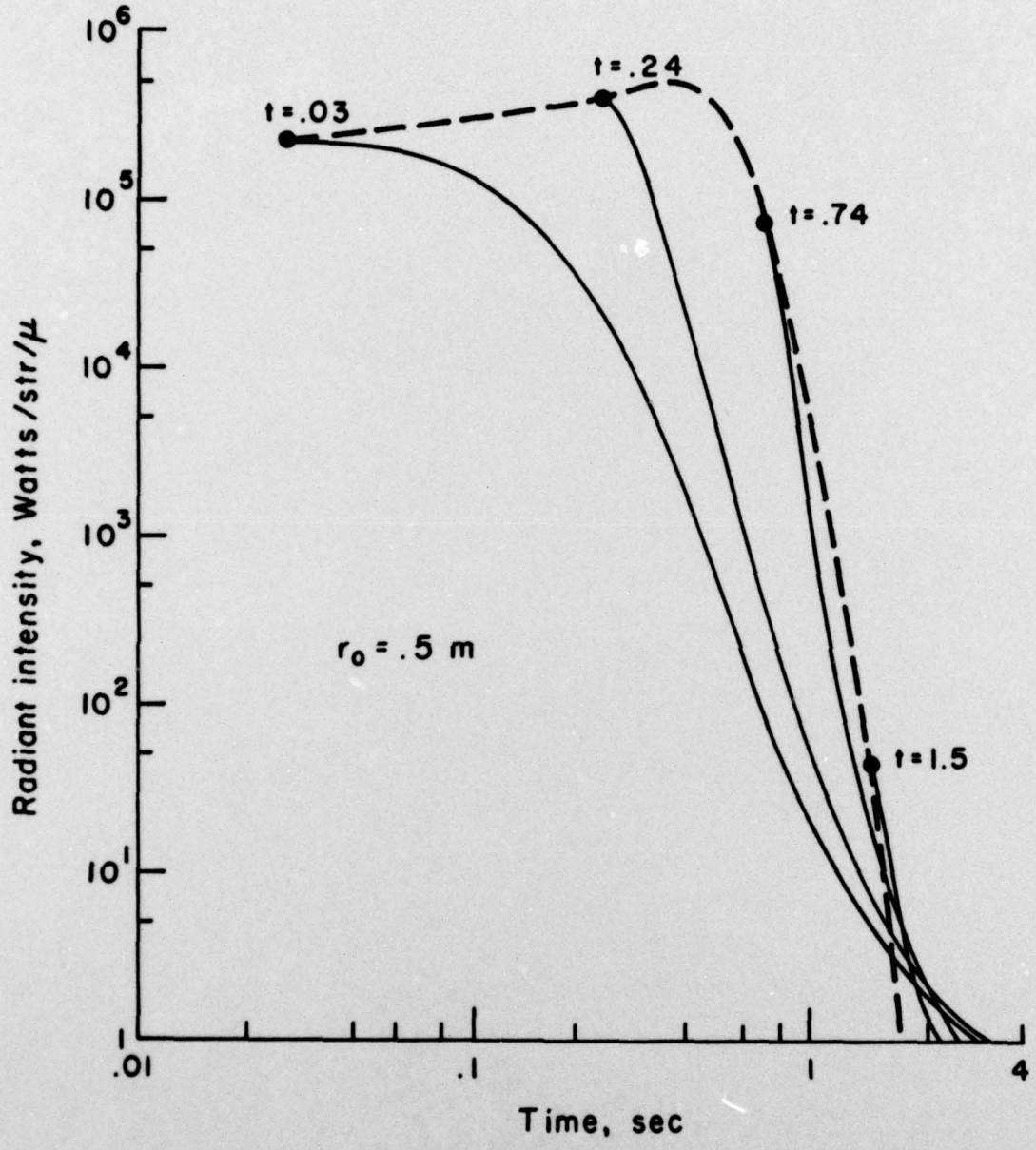

Figure 16. Radiation time history at various ignition points for a 1 meter diameter hydrogen bubble starting from rest.

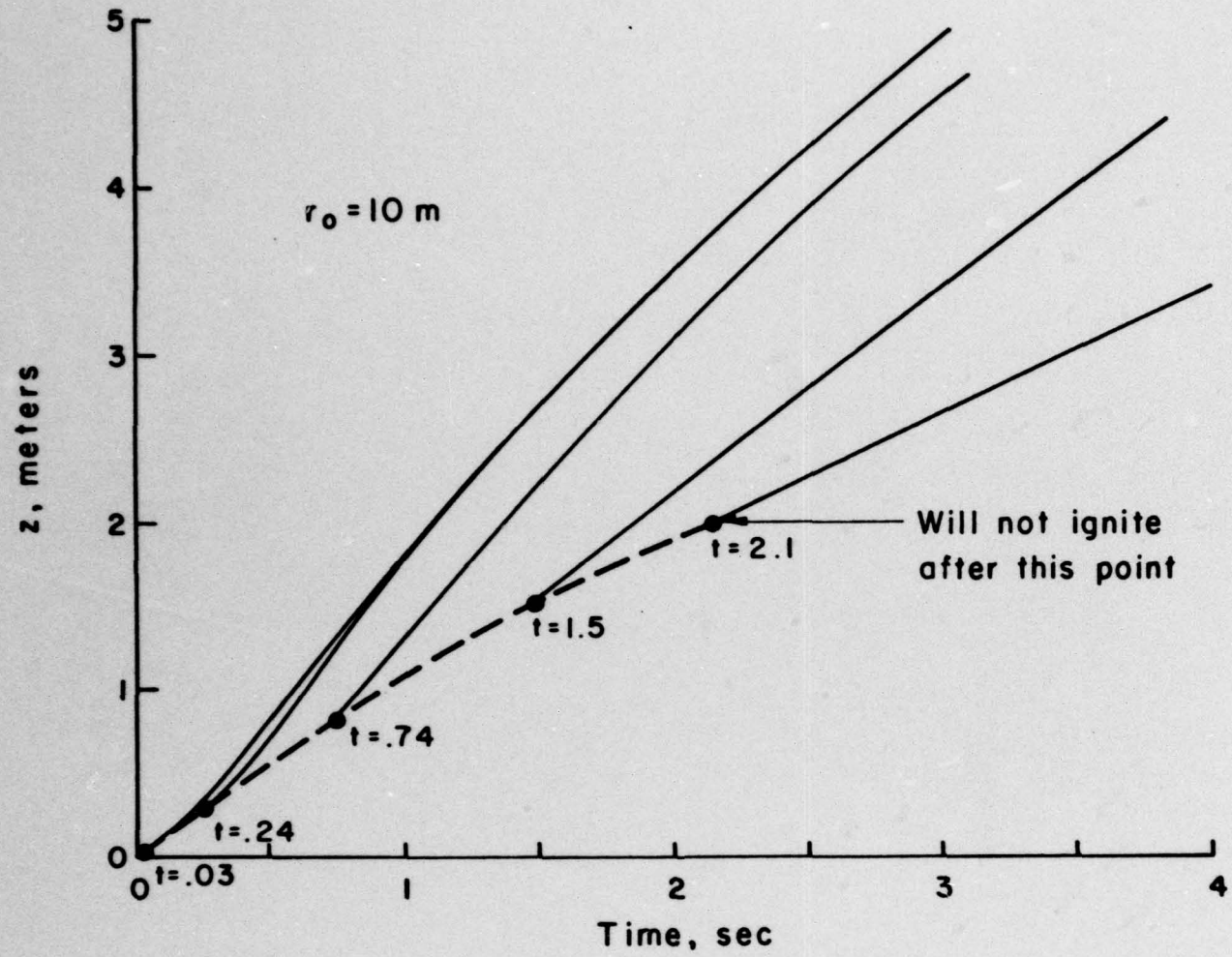

Figure 17. Altitude time history at various ignition points for a 20 meter diameter hydrogen bubble starting from rest.

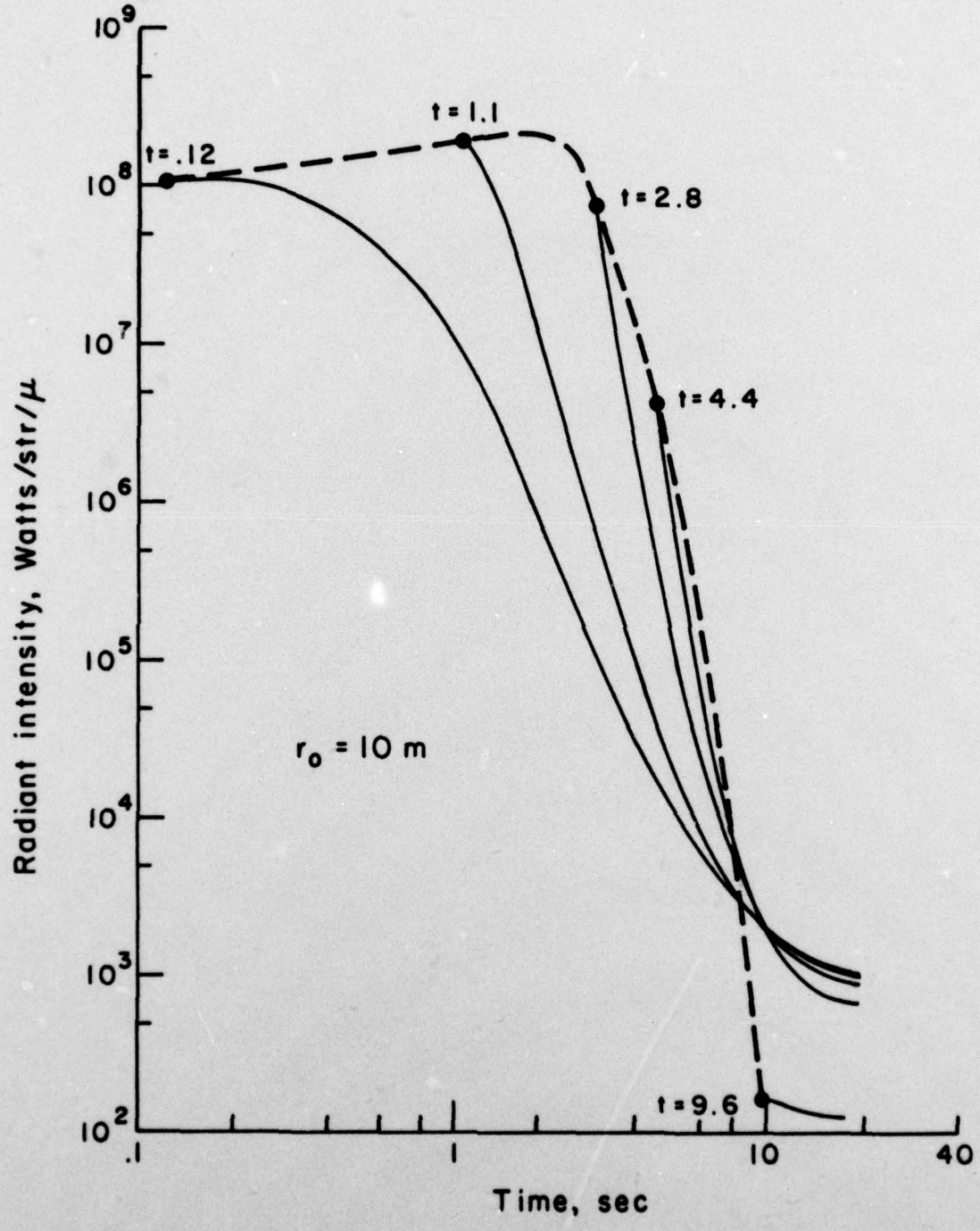

Figure 18. Radiation time history at various ignition points for a 20 meter diameter hydrogen bubble starting from rest.

5. SUMMARY

The motion of buoyant gas clouds has been examined using the simplified model found in References 1 and 5. The effect of a crosswind on bubble motion is also treated but is found to have negligible effect. Comparison of the model with data on small hydrogen bubbles at ambient temperature, hot combusted CH_4-O_2 clouds, and thermals caused by nuclear explosions indicates that the model is applicable to a wide variety of bubble types with the appropriate choice of entrainment coefficient. Since there is not sufficient data at this time to conclusively determine the entrainment coefficient suitable for large H_2 bubbles, the entrainment coefficient measured by Gorev et al. for small hydrogen bubbles ($\alpha = .41$) is used.

Gorev et al. ignited H_2 bubbles at various altitudes and measured the volume of the combustion products at these different mixture ratios. The degree of expansion predicted by total combustion of a homogenous mixture differs considerably from the data since the bubble is never mixed on a microscopic scale and burns with the surrounding air when fuel rich. A semi-empirical theory was developed whereby parameters of the combustion process such as percentage of H_2 burned and temperature after ignition could be obtained from a model which maintained the observed expansion. It was found that the temperature of the cloud after ignition is highest if the bubble is ignited just before it reaches a stochiometric mixture ratio. In addition, the more fuel rich the mixture, the greater the percentage of hydrogen which is converted into water.

A lower and upper limit to the radiation is obtained by applying the radiation model developed by Fishburne[13] to bubbles in which the combustion products and unreacted species are either thoroughly mixed or unmixed, respectively. The time history of the radiation after ignition as the bubble cools is also examined and compared with data on combusted CH_4-O_2 clouds. Radiative loss and recombination were also included, but seem to have only a small effect. The entrainment coefficient is a much more sensitive parameter. The model was applied to H_2 bubbles after ignition as well. A

20 meter diameter bubble was seen to have a peak radiation of 10^8 watts/str/μ if ignited within several seconds after release while still in the fuel rich domain. However, after 10 seconds and at an altitude of 40 meters, the bubble becomes so fuel lean that it can no longer be ignited. The smallest bubble considered (a diameter of 1 meter) cannot be ignited after only 2.2 seconds or above an altitude of 2 meters. It thus reaches its peak radiation of 10^5 watts/str/μ only if ignited within .6 second after release. The radiation of the hot combustion products drops off very rapidly after ignition. Even for the 20 meter diameter bubble, the maximum time in which a significant radiation signature is sustained is 8 seconds.

6. REFERENCES

1. V.A. Gorev, P.A. Gusev, and Ya. K. Troshin, Dokl. Akad. Nauk, 222 No. 4, 539 (1975).

2. R.A. Bigoni and D.A. Matuska, "Preliminary Report on Project Gas Explosive Simulation Technique (GEST)," AFWL-TR-74-252 (1974).

3. C.P. Wang, Phys. Fluids 14, 1643 (1971).

4. C.P. Wang, Phys. Fluids 16, 744 (1973).

5. V.H. Shui and G.M. Weyl, Phys. Fluids 18, 15 (1975).

6. B.P. Sanford and R.J. Huppi, "GEST Infrared Spectra at 1.56 to 4.67 Microns," Preliminary Report, Air Force Cambridge Research Laboratories, Bedford, Mass. 01730, (March 1974).

7. R.S. Scorer, J. Fluid Mech. 2, 583 (1957).

8. J.S. Turner, "Annual Review of Fluid Mechanics," edited by W.R. Sears and M. Van Dyke (Annual Reviews, Palo Alto, Calif. 1969), Vol 1. p.29.

9. W.G. Brown and D.L. Warlick, "Properties of Combustion Gases, System: H_2-Air, Equilibrium Compositions, Thermodynamic Properties," Flight Propulsion Division, General Electric, Cincinnati, Ohio 45213 (Sept. 1964).

10. D.R. Cruise, "Information Manual for the Theoretical Propellant Evaluation Program," Naval Weapons Center PEP NOTE TN-U-1 (plus additions), (December 1964).

11. JANNAF Thermochemical Tables (Dow Chemical Company, Midland, Mich.), continuously updated.

12. V.A. Gorev, P.A. Gusev, and Ya. K. Troshin, FTD-ID(RS)I-0208-76, p. 5 (1975).

13. E.S. Fishburne, "Factors Influencing the Scaling of Thrust with Infrared Radiation," JANNAF 9th Plume Technology Meeting (Feb. 1976).

14. R.A. Martinsen and E.S. Fishburne, "A Fine Spectral Resolution (FSR) Program for the Calculation of Infrared Radiation Emitted by Exhaust Plumes," Grumman Research Department Memorandum RM-575 (July 1973).

15. H.C. Hottel, Chapter 2 of Heat Transmission (by W.C. McAdams), 3d ed. McGraw-Hill Book Company, Inc., New York (1954).